# Maximum Principle Preserving Schemes for Interface Problems with Discontinuous Coefficients

Zhilin Li and Kazufumi Ito
Center for Research in Scientific Computation
& Department of Mathematics
North Carolina State University
Raleigh, NC 27695
zhilin@math.ncsu.edu & kito@math.ncsu.edu

**Abstract**

New finite difference methods using Cartesian grids are developed for elliptic interface problems with variable discontinuous coefficients, singular sources, and non-smooth or even discontinuous solutions. The new finite difference schemes are constructed to satisfy the sign property of the discrete maximum principle using quadratic optimization techniques. Convergence proofs are provided for the first and second order methods by constructing comparison functions. The methods are coupled with a multigrid solver. Numerical examples are also provided to show the efficiency of the proposed methods.

**Key words.** Elliptic equation, finite difference methods, irregular domain, interface, discontinuous coefficients, singular source term, delta functions, quadratic optimization, multigrid method

**AMS subject classifications.** 65N06, 65N50

## 1 Introduction

Many important practical problems lead to partial differential equations whose solutions have discontinuities or non-smoothness across some interfaces within the solution domains. In this paper, we propose a class of numerical methods that preserve the discrete maximum principle for the interface problems defined below:

$$(\beta u_x)_x + (\beta u_y)_y - \kappa(x,y)\, u = f(x,y), \qquad (x,y) \in \Omega = \Omega^+ \cap \Omega^-, \tag{1.1}$$

with a boundary condition on $\partial\Omega$, where $\beta$, $\kappa$ and $f$ are piecewise continuous and may have jump discontinuity across some curve $\Gamma$ in the domain $\Omega$, $f$ can also contain singular sources as reflected in the following jump conditions:

$$[u]_{|\mathbf{X}\in\Gamma} = w(s), \qquad [\beta u_n]_{|\mathbf{X}\in\Gamma} = v(s), \tag{1.2}$$

where the jump is defined as the difference of the limiting values of two different sides of the interface, for example

$$[u]_{|\mathbf{X}\in\Gamma} = \lim_{\mathbf{x}\to\mathbf{X},\mathbf{X}\in\Omega^+} u(\mathbf{x}) - \lim_{\mathbf{x}\to\mathbf{X},\mathbf{X}\in\Omega^-} u(\mathbf{x}),$$

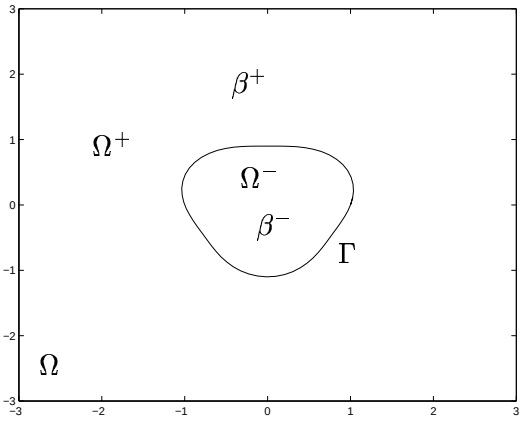


Figure 1: (a). A diagram of a rectangular domain $\Omega = \Omega^+ \cup \Omega^-$ with an immersed interface $\Gamma$. The coefficients $\beta(\mathbf{x})$ may have a jump across the interface.

see Fig. 1 for an illustration. The interface $\Gamma$ can be an arbitrary piecewise smooth curve lying in $\Omega$. We need not assume that $\Gamma$ is closed or even connected. In the case that $\kappa$ is continuous and $w(s) \equiv 0$, the interface problem can be written as a boundary value problem below:

$$\nabla \cdot (\beta \nabla u) - \kappa\, u = f + \int_\Gamma v(s)\delta_2(\mathbf{x} - X(s))ds, \qquad (x, y) \in \Omega,$$
$$\text{given boundary condition on} \quad \partial\Omega,$$

where $\delta_2$ is the two dimensional Dirac delta function which is singular, the second term at the right hand side is a distribution which satisfies

$$\iint_\Omega \int_\Gamma v(s)\delta_2(\mathbf{x} - X(s))\Psi(x, y)dxdyds = \int_\Gamma v(s)\Psi(X(s), Y(s))ds \tag{1.3}$$

for any arbitrary smooth function $\Psi(x, y)$. The discussion of the existence and the regularity of the solution can be found, for example, in [2, 6]. Generally, if $\beta$, $\kappa$, and $f$ are piecewise continuous in $\Omega$, and $w$ and $v$ are continuous along $\Gamma$, then the solution to the interface problem exists and it is in $H^2(\Omega)$.

There are several numerical methods in the literature designed for the interface problems discussed in this paper. We just mention a few here: the finite element methods using body fitting grids [6, 35]; the fast solvers based on integral equations for piecewise constant coefficients [10, 25, 26, 27] including the fast multipole method; the first order ghost fluid method [24]. In this paper, our new methods are based on the local immersed interface method (IIM) [15, 18].

The immersed interface method [15, 18] was originally designed for elliptic equations having discontinuous coefficients and singular source terms due to interfaces in the solution domain. Intended to improve Peskin's immersed boundary method (IBM) [30, 31], which is a first order method using discrete delta functions, the immersed interface method can be used to deal with discontinuous coefficients and singular sources simultaneously by using known jump conditions. The essence of the IIM includes: ***(a)*** using uniform or adaptive Cartesian grids, therefore there is almost no cost in the grid generation since Cartesian grids are fixed. This is very significant for moving interface/free boundary problems, or problems with complicated geometries, or problems with topological changes, because the grid generation process may be the most expensive part

in an entire simulation. Another advantage using Cartesian grids is that we can take advantage of many software packages or methods developed for Cartesian grids, for example, fast Poisson solvers [32], Clawpack [14], Amrclawpack [3], the level set method [29], algebraic multi-grid solvers [1, 8], and many others. ***(b)*** using standard numerical methods away from interfaces where there are no irregularities; ***(c)*** taking into account the known jump conditions, usually in the solutions and fluxes, in deriving numerical schemes at grid points near or on interfaces to keep the global accuracy unaffected by the presence of the interfaces; ***(d)*** introducing non-zero correction terms to balance the singular source terms. The IIM gives sharp solutions (no smear-out) across the interfaces since the jump conditions are enforced. Generally the IIM uses only local information, specifically, the partial differential equations (PDE), the jump conditions, the interface, and the underlying grid. Pointwise second order accuracy is either proved or confirmed in further development of the method and applications, see for example, [5, 9, 12, 16, 19, 20, 34]., The IIM has been successfully coupled with evolution schemes such as the particle approach and the level set method for moving interface and free boundary problems [11, 13, 17, 22, 23].

The original immersed interface method provides a new approach to discretize interface problems to second order accuracy. The method is very successful and has been applied to many problems. However, for variable coefficients with jumps, the resulting linear system of equations from the IIM is not symmetric positive definite. While it is stable for one dimensional problems and certain two dimensional problems [12], the stability of the algorithm depends on the choice of one or more extra grid points in addition to the standard finite difference stencil [9]. Various attempts have been made to speed up the process for solving the resulting linear system and improve the stability of the original immersed interface method, for example, the multigrid method by L. Adams [1]; the explicit jump immersed interface method by Wiegmann [33] and some others. For the special case when $\beta$ is ***piecewise constant***, the fast iterative method proposed in [20] is very successful and efficient [11, 23, 22].

In this paper, we will develop new methods for ***arbitrary*** $\beta(x, y)$ ***using direct finite difference discretization***. The new methods satisfy the sign property that guarantees the discrete maximum principle. The sign property is enforced through a constrained quadratic optimization problem. The resulting linear system of equations from the finite difference methods is diagonally dominant and its symmetric part is negative definite. Two typical finite difference schemes using the optimization approach are specifically discussed. One is a first order method that uses the standard five-point stencil. The other one is a second order method that uses a standard nine-point stencil. Proofs of the convergence and error estimates of these two methods are provided. For the second order method that uses a standard nine-point stencil, we use multigrid solvers developed in [1] and [8] to solve the resulting linear system of equations. The generalization of the methods to non self-adjoint elliptic, parabolic equations, and three dimensional problems, are under consideration.

The idea in this paper actually was proposed and tested by Z. Li (1993), S. Moskow and F. Santosa (1996-1997). But due to various reasons, it has never been written up and published.

The paper is organized as follows. In Section 2, we lay down some theoretical fundamentals for interface problems that are needed in deriving the new methods. Then we derive the new methods using optimization techniques in Section 3. Convergence analysis for the first order and second order methods are given in Section 4 and 5 respectively. The numerical results are presented in Section 6. In Appendix, we present an integral equation for the solution of the interface problems with piecewise constant coefficients and a regularity result of solutions.

# 2 Preliminaries

## 2.1 The local coordinates and the jump relations

Given a point $(X, Y)$ on the interface, it is sometimes convenient to use the local coordinates in the normal and the tangential directions:

$$\begin{aligned} \xi &= (x - X)\cos\theta + (y - Y)\sin\theta, \\ \eta &= -(x - X)\sin\theta + (y - Y)\cos\theta, \end{aligned} \tag{2.4}$$

where $\theta$ is the angle between the $x$-axis and the normal direction, pointing in the direction of a specified side, say the + side in Fig. 2.1. We use the superscripts $-$ or $+$ to denote the limiting values of a function from one side or the other. Under the local coordinates, the limiting differential equation approaching to the interface from a particular side, for example, from the $-$ side, can be written

$$\beta^- \left(u^-_{\xi\,\xi} + u^-_{\eta\,\eta}\right) + \beta^-_\xi u^-_\xi + \beta^-_\eta u^-_\eta - k^- u^- = f^-. \tag{2.5}$$

At the point $(X, Y)$, the interface can be written as

$$\xi = \chi(\eta), \quad \text{with} \quad \chi(0) = 0, \quad \chi'(0) = 0. \tag{2.6}$$

The curvature of the interface at $(X, Y)$ is $\chi''$.

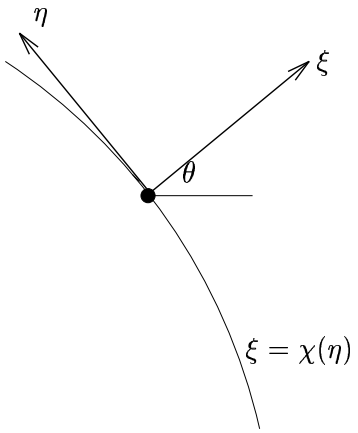


Figure 2: A diagram of the local coordinates in the normal and tangential directions, where $\theta$ is the angle between the $x$-axis and the normal direction.

## 2.2 Interface relations

From the jump conditions (1.2) and the partial differential equation (1.1), we have derived the following interface relations in [15, 18] that represent the limiting quantities from one side in terms of the other.

**Theorem 2.1** *Let $u(x, y)$ be the solution to (1.1) and (1.2). Let $(X, Y)$ be a point on the interface. Define $\rho = \beta^+/\beta^-$. Then there are the following interface relations under the local*

*coordinates (2.4).*

$$
\begin{aligned}
u^+ &= u^- + w, \\
u^+_\xi &= \rho\, u^-_\xi + \frac{v}{\beta^+}, \\
u^+_\eta &= u^-_\eta + w', \\
u^+_{\xi\xi} &= \left(\frac{\beta_\xi{}^-}{\beta^+} - \chi''\right) u^-_\xi + \left(\chi'' - \frac{\beta_\xi{}^+}{\beta^+}\right) u^+_\xi + \frac{\beta_\eta{}^-}{\beta^+}\, u^-_\eta - \frac{\beta_\eta{}^+}{\beta^+}\, u^+_\eta \\
&\qquad + (\rho - 1)\, u^-_{\eta\eta} + \rho u^-_{\xi\xi} - w'' + \frac{[f]}{\beta^+} + \frac{[\kappa]\, u^- + \kappa^+\, [u]}{\beta^+}, \\
u^+_{\eta\eta} &= u^-_{\eta\eta} + (u^-_\xi - u^+_\xi)\, \chi'' + w'', \\
u^+_{\xi\eta} &= \frac{\beta_\eta{}^-}{\beta^+}\, u^-_\xi - \frac{\beta_\eta{}^+}{\beta^+} u^+_\xi + \left(u^+_\eta - \rho u^-_\eta\right) \chi'' + \rho\, u^-_{\xi\eta} + \frac{v'}{\beta^+}.
\end{aligned}
\tag{2.7}
$$

These interface relations are used in deriving the new finite difference method in the next section.

# 3 Algorithm description

We assume the domain $\Omega$ is a rectangle, say $[a, b] \times [c, d]$. We take a uniform grid with

$$x_i = a + ih_x,\ y_j = a + jh_y,\ \ i = 0, 1, \cdots, m, \quad j = 0, 1, \cdots, n,$$

where $h_x = (b - a)/m$ and $h_y = (d - c)/n$.

Our goal is to develop a finite difference equation of the form

$$\sum_k^{n_s} \gamma_k\, U_{i+i_k, j+j_k} - \kappa_{ij}\, U_{ij} = f_{ij} + C_{ij} \tag{3.8}$$

for use at any grid point $(x_i, y_j)$, where $n_s$ is the number of grid points in the finite difference stencil, and $U_{ij}$ is the approximation to the solution $u(x, y)$ of (1.1) and (1.2) at $(x_i, y_j)$. The sum over $k$ involves a finite numbers of points neighboring $(x_i, y_j)$. So each $i_k, j_k$ will take values in the set $\{0, \pm 1, \pm 2 \cdots\}$. The coefficients $\gamma_k$ and the indices $i_k, j_k$ will depend on $(i, j)$, so these should really be labeled $\gamma_{ijk}$, etc., but for simplicity of notation we will concentrate on a single grid point $(x_i, y_j)$ and drop these indices.

The local truncation error at a grid point $(x_i, y_j)$ is defined as

$$T_{ij} = \sum_k^{n_s} \gamma_k\, u\left(x_{i+i_k}, y_{j+j_k}\right) - \kappa_{ij}\, u(x_i, y_j) - f(x_i, y_j) - C_{ij} \tag{3.9}$$

We say $(x_i, y_j)$ is a *regular point* if the interface does not come between any points in the standard five-point stencil centered at $(i, j)$. At these points we obtain an $O(h^2)$ truncation error

using the standard 5-point ($n_s = 5$) formula

$$\frac{1}{h_x}\left(\beta_{i+1/2,j}\frac{(u_{i+1,j}-u_{ij})}{h_x} - \beta_{i-1/2,j}\frac{(u_{i,j}-u_{i-1,j})}{h_x}\right) + \frac{1}{h_y}\left(\beta_{i,j+1/2}\frac{(u_{i,j+1}-u_{i,j})}{h_y} - \beta_{i,j-1/2}\frac{(u_{i,j}-u_{i,j-1})}{h_y}\right) - \kappa_{ij}u_{ij} = f_{ij}, \tag{3.10}$$

with

$$C_{ij} = 0, \tag{3.11}$$

where

$$\beta_{ij} = \beta(x_i, y_j), \quad \beta_{i+\frac{1}{2},j} = \beta\left(x_i + \frac{h_x}{2}, y_j\right),$$

and so on.

We wish to determine formulas of the form (3.8) for *irregular grid points* around which the standard five-point stencil contains grid points from both sides of the interface. First we choose a point $(x_i^*, y_j^*)$ on the interface $\Gamma$ near the grid point $(x_i, y_j)$. Usually, we take $(x_i^*, y_j^*)$ as the projection of $(x_i, y_j)$ on the interface or the intersection of the interface and one of axes. We then expand each $u(x_{i+i_k}, y_{j+j_k})$ about $(x_i^*, y_j^*)$ under the local coordinates, being careful to use the limiting values of derivatives of $u$ from the correct side of the interface.

$$u(x_{i+i_k}, y_{j+j_k}) = u(\xi_k, \eta_k) = u^{\pm} + \xi_k u_\xi^{\pm} + \eta_k u_\eta^{\pm} + \frac{1}{2}\xi_k^2 u_{\xi\xi}^{\pm} + \xi_k\eta_k u_{\xi\eta}^{\pm} + \frac{1}{2}\eta_k^2 u_{\eta\eta}^{\pm} + O(h^3), \tag{3.12}$$

where the $+$ or $-$ sign is chosen depending on whether $(\xi_k, \eta_k)$ lies on the $+$ or $-$ side of $\Gamma$.

If we do this expansion at each point used in the finite difference equation (3.8) then the local truncation error $T_{ij}$ can be expressed as a linear combination of the values $u^{\pm}$, $u_\xi^{\pm}$, $u_\eta^{\pm}$, $u_{\xi\xi}^{\pm}$, $u_{\xi\eta}^{\pm}$, $u_{\eta\eta}^{\pm}$ as the following,

$$\begin{aligned} T_{ij} \;=\; & a_1\,u^- + a_2\,u^+ + a_3\,u_\xi^- + a_4\,u_\xi^+ + a_5\,u_\eta^- + a_6 u_\eta^+ + a_7\,u_{\xi\,\xi}^- + a_8\,u_{\xi\,\xi}^+ \\ & + a_9\,u_{\eta\eta}^- + a_{10}\,u_{\eta\eta}^+ + a_{11}\,u_{\xi\,\eta}^- + a_{12}\,u_{\xi\,\eta}^+ - \kappa^- u^- - f^- - C_{ij} + \cdots . \end{aligned} \tag{3.13}$$

The quantities $f^{\pm}$, $\kappa^{\pm}$, $\beta^{\pm}$ are the limiting values of the functions at $(x_i^*, y_j^*)$ from $+$ side or $-$ side of the interface. The coefficients $a_j$ depend only on the position of the stencil relative to the interface. They are independent of the functions $u, \kappa$ and $f$. If we define the index sets $K^+$ and $K^-$ by

$$K^{\pm} = \{k : \ (\xi_k, \eta_k) \text{ is on the } \pm \text{ side of } \Gamma\},$$

then the $a_j$ are given by

$$
\begin{aligned}
a_1 &= \sum_{k\in K^-} \gamma_k & a_2 &= \sum_{k\in K^+} \gamma_k \\
a_3 &= \sum_{k\in K^-} \xi_k\gamma_k & a_4 &= \sum_{k\in K^+} \xi_k\gamma_k \\
a_5 &= \sum_{k\in K^-} \eta_k\gamma_k & a_6 &= \sum_{k\in K^+} \eta_k\gamma_k \\
a_7 &= \frac{1}{2}\sum_{k\in K^-} \xi_k^2\gamma_k & a_8 &= \frac{1}{2}\sum_{k\in K^+} \xi_k^2\gamma_k \\
a_9 &= \frac{1}{2}\sum_{k\in K^-} \eta_k^2\gamma_k & a_{10} &= \frac{1}{2}\sum_{k\in K^+} \eta_k^2\gamma_k \\
a_{11} &= \sum_{k\in K^-} \xi_k\eta_k\gamma_k & a_{12} &= \sum_{k\in K^+} \xi_k\eta_k\gamma_k.
\end{aligned}
\tag{3.14}
$$

Using the interface relations (2.7), we eliminate the quantities from one side, say, the + side using the quantities from the other side, say, the − side, collect terms to get an expression of the form[1]

$$
\begin{aligned}
T_{ij} \;=\;& \left(a_1 + \frac{a_8\,[\kappa]}{\beta^+} + a_2\right) u^- + \left\{ a_3 + a_8\left(\frac{{\beta_\xi}^-}{\beta^+} - \chi''\right) + a_{10}\chi'' + a_{12}\frac{{\beta_\eta}^-}{\beta^+} \right. \\
& \left. +\rho\left(a_4 + a_8\left(\chi'' - \frac{{\beta_\xi}^+}{\beta^+}\right) - a_{10}\chi'' - a_{12}\frac{{\beta_\eta}^+}{\beta^+}\right) - {\beta_\xi}^- \right\} u_\xi^- \\
& + \left\{ a_5 + a_6 + a_8\left(\frac{{\beta_\eta}^-}{\beta^+} - \frac{{\beta_\eta}^+}{\beta^+}\right) + a_{12}(1-\rho)\,\chi'' - {\beta_\eta}^- \right\} u_\eta^- \\
& + \left\{a_7 + a_8\rho - \beta^-\right\} u_{\xi\,\xi}^- + \left\{a_9 + a_{10} + a_8\,(\rho-1) - \beta^-\right\} u_{\eta\,\eta}^- \\
& + \left\{a_{11} + a_{12}\rho\right\} u_{\xi\,\eta}^- - \kappa^- u^- - f^- + (\hat{T}_{ij} - C_{ij}) + \cdots,
\end{aligned}
\tag{3.15}
$$

where

$$
\begin{aligned}
\hat{T}_{ij} \;=\;& a_2\,w + a_{12}\,\frac{v'}{\beta^+} + \left(a_6 - \frac{a_8\,{\beta_\xi}^+}{\beta^+} + a_{12}\chi''\right) w' \\
& + a_{10}\,w'' + \frac{1}{\beta^+}\left(a_4 + a_8(\chi'' - \frac{{\beta_\xi}^+}{\beta^+}) - a_{10}\chi'' - a_{12}\frac{{\beta_\eta}^+}{\beta^+}\right) v \\
& + a_8\left\{\frac{[f]}{\beta^+} + \frac{\kappa^+ w}{\beta^+} - w''\right\}.
\end{aligned}
\tag{3.16}
$$

Although the local truncation errors do not tell the whole story about the global error due to the cancellation of errors, we can guarantee certain accuracy of the computed solution by requiring

[1] A more subtle approach is to expand all $u(x_{i+i_k}, y_{j+j_k})$ at the grid point $(x_i, y_j)$. If $(x_{i+i_k}, y_{j+j_k})$ is a grid point on the different side from $(x_i, y_j)$, we can first expand $u(x_{i+i_k}, y_{j+j_k})$ at a point $(x_i^*, y_j^*)$ on the interface; then express all the quantities up to second order derivative in terms of the those on the other side using the jump relations (2.7); expand those quantities again at $(x_i, y_j)$. This approach gives slight better results (small error constant). However, for simplicity, we will use the equation on the point $(x_i^*, y_j^*)$ from a particular side.

some of coefficients of $u^-$, $u_\xi^-$, $u_\eta^-$, $\cdots$ vanish:

$$\begin{aligned}
a_1 + a_2 + a_8 \frac{[\kappa]}{\beta^+} &= 0 \\
a_3 + \rho a_4 + a_8 \frac{\beta_\xi{}^- - \rho \beta_\xi{}^+ - [\beta]\chi''}{\beta^+} + a_{10} \frac{[\beta]\chi''}{\beta^+} + a_{12} \frac{\beta_\eta{}^- - \rho \beta_\eta{}^+}{\beta^+} &= \beta_\xi{}^- \\
a_5 + a_6 - a_8 \frac{[\beta_\eta]}{\beta^+} + a_{12}(1-\rho)\,\chi'' &= \beta_\eta{}^- \\
a_7 + a_8\,\rho &= \beta^- \\
a_9 + a_{10} + a_8\,(\rho - 1) &= \beta^- \\
a_{11} + a_{12}\,\rho &= 0,
\end{aligned} \tag{3.17}$$

where $\rho = \beta^-/\beta^+$. Once the $\gamma_k$'s are computed, we can easily obtain $C_{ij}$ as

$$C_{ij} = \hat{T}_{ij} \tag{3.18}$$

where $\hat{T}_{ij}$ is given by (3.16).

### 3.1 An optimization approach

In order to obtain finite difference schemes that satisfy the discrete maximum principle, see Section 6.5 of Morton and Mayers [28] for the definition, we need to impose the sign restriction on the coefficients $\gamma_k$ in (3.8)

$$\begin{aligned}
\gamma_k \geq 0 \quad &\text{if} \quad (i_k, j_k) \neq (0,0), \\
\gamma_k < 0 \quad &\text{if} \quad (i_k, j_k) = (0,0),
\end{aligned} \tag{3.19}$$

along with several equations in (3.17). At regular grid points, the standard central finite difference scheme satisfies the sign restriction and the equations in (3.17). So we will only concentrate our discussion on a typical irregular grid point $(x_i, y_j)$. We form the following constrained quadratic optimization problem to determine the coefficients of the finite difference scheme

$$\min_\gamma \left\{ \frac{1}{2} \gamma^T H \gamma - \gamma^T g \right\}, \tag{3.20}$$

$$s.t. \qquad A\gamma = b, \quad \gamma_k \geq 0, \quad \text{if} \quad (i_k, j_k) \neq (0,0) \quad \gamma_k < 0, \quad \text{if} \quad (i_k, j_k) = (0,0), \tag{3.21}$$

where $\gamma = [\,\gamma_1, \gamma_2, \cdots,\,]^T$ is the vector composed of the coefficients of the finite difference scheme, $H$ is a symmetric positive definite matrix and $g \in R^{n_s}$. $A\gamma = b$ is the system of linear equations that contains several or all equations in (3.17). Naturally we want to choose $\gamma_k$ in a such a way that they become the coefficients of the standard 5-point central difference scheme if there is no interface. This can be done by minimizing

$$\min_\gamma \frac{1}{2} \sum_k (\gamma_k - g_k)^2, \tag{3.22}$$

where

$$\begin{aligned} g_k &= \frac{2\beta_{i+i_k,j+j_k}}{h_x^2+h_y^2}, \quad (i_k,j_k) \in \{(-1,0),(1,0),(0,-1),(0,1)\}, \\ g_k &= -\frac{8\beta_{i,j}}{h_x^2+h_y^2}, \quad (i_k,j_k) = (0,0), \\ g_k &= 0, \quad \text{Otherwise.} \end{aligned} \tag{3.23}$$

The matrix $H$ in (3.20) is then the identity matrix. Another choice of $g$ is $g = A^+ b$, where $A^+$ is the pseudo-inverse of $A$, and $g = A^+ b$ is the least squares solution to the system of equations $Ax = b$. We can also choose some combination of (3.23) and $A^+ b$.

There are two parameters in the optimization algorithm (3.20)-(3.21) that are to be determined. The first one is $n_s$, the number of grid points involved in the finite difference scheme. The second one is the number of equations from (3.17) that to be satisfied in (3.21). We will discuss two different methods in this paper.

### 3.2 First order methods

If we wish to get a simple first order method, then we can use the first three equations in (3.17). In this case, as we will show later, we can take $n_s = 5$, and the standard five-point stencil

$$\{(i_1,j_1),(i_2,j_2),(i_3,j_3),(i_4,j_4),(i_5,j_5)\} = \{(-1,0),(0,0),(1,0),(0,-1),(0,1)\}. \tag{3.24}$$

The optimization problem can be constructed as:

$$\min_{\gamma} \left\{ \frac{1}{2}\gamma^T H \gamma - \gamma^T g + \sum_{l=4}^{6} w_l \left(A_l \gamma - b_l\right)^2 \right\}, \tag{3.25}$$

$$s.t. \quad \begin{bmatrix} A_1 \\ A_2 \\ A_3 \end{bmatrix} \gamma = b, \quad \gamma_k \geq 0, \quad \text{if} \quad (i_k,j_k) \neq (0,0) \quad \gamma_k < 0, \quad \text{if} \quad (i_k,j_k) = (0,0), \tag{3.26}$$

where $A_l\gamma = b_l$, $1 \leq i \leq 6$, is the $l$-th equation in (3.17), $w_l$ are pre-defined weights for $l = 4,5,6$.

Since the high order terms have little effect on the convergence order, we can neglect them to get simplified equality and inequality constraints

$$\begin{aligned} a_1 + a_2 + a_8 \frac{[\kappa]}{\beta^+} &= 0 \\ a_3 + \rho a_4 &= {\beta_\xi}^- \\ a_5 + a_6 &= {\beta_\eta}^- \\ \gamma_k \geq 0, \quad k \neq 2, \qquad \gamma_2 &\leq 0. \end{aligned} \tag{3.27}$$

Even though the local truncation errors at irregular grid points using the first order method are $O(1)$, the global error is $O(h)$ as we will show later.

### 3.3 Second order methods

In order to get second order methods, we require all the six equations in (3.17) to be satisfied plus the sign restriction (3.19) for the optimization problem. Therefore $n_s \geq 6$. It is not clear what the smallest $n_s$ is. The hint is from the conforming finite element method for interface problems with a uniform triangulation [21]. The implementation is somewhat complicated for the conforming finite element method though. The analysis there suggests a non-standard nine-point stencil for the finite element method that guarantees the stiffness matrix to be symmetric positive definite. Since we do not require the symmetry in the linear system of the finite difference equations described in this paper, we should expect that the minimum $n_s$ needed for the optimization problem to have solutions is $n_s \leq 9$ if $h_x$ and $h_y$ are small enough. Thus we can take a standard nine-point stencil. Our numerical experiments showed that it is enough to have an eight-point stencil provide that we carefully choose additional three grid points in addition to the standard five-point stencil. Usually we should choose the additional grid points close to the interface as the finite element method suggested. However, a more robust choice is the standard nine-point stencil, $n_s = 9$, and the resulting linear finite difference system of equations is still block tridiagonal. If we use the standard nine-point stencil, $n_s = 9$, the $k$, $i_k$, and $j_k$ can be determined by the following loop

```
k = 1
for i_k = -1,1
   for j_k = -1, 1
      k = k + 1
   end
end
```

Later we will numerically prove the existence of the solution to the optimization problem.

### 3.4 Solving the optimization problems

There are several commercial and educational software packages that are designed to solve constrained quadratic optimization problems. For example, the ***QP*** function in Matlab; the ***QL*** program in Fortran computer language developed by K. Schittkowski; and the ***IQP*** Fortran code from ***Port*** managed by Lucent Technology.

Most of quadratic optimization solves require users to provide the initial guess, the lower and upper bounds and other information. In our method, we take the initial guess as the vector $g$, and the lower and upper bounds as

$$0 < \gamma_k < \frac{2\,\beta_{\max}}{h_x^2 + h_y^2}, \quad \text{if} \quad (i_k, j_k) \neq (0,0); \qquad -\frac{8\,\beta_{\max}}{h_x^2 + h_y^2} < \gamma_k < 0, \quad \text{if} \quad (i_k, j_k) = (0,0), \tag{3.28}$$

where $\beta_{\max}$ is an estimation of the upper bound of the coefficient $\beta(x, y)$. Since the size of the optimization problem is very small, the total cost in solving the associated optimization problems is only a small portion compared with that needed for solving the global resulting linear system of equations. Our preliminary tests using the FFT or multi-grid solver for the linear system of equations show that the extra time needed in dealing with the interface including solving the optimization problem is only about 5-8% in the entire solution process, see Sec. 6.2.

In case that the optimization solver fails to give a solution or provides a wrong solution, we can either add a few more grid points that are closer to the interface or switch to another scheme that satisfies the discrete maximum principle at the particular grid point such as the ghost fluid or the smoothing method, without affecting global accuracy. As we will show later, if the optimization solver fails to return a feasible solution, it usually means the grid resolution is too low and the interface cuts the grid lines more than twice meaning the curvature is very large relative to the underlying grid. In our numerical tests, such failure has never happened for second order methods with reasonable grids.

# 4 Convergence analysis for the first order method

In this section, we show some theoretical results for the first order method using a standard five-point stencil. First we prove the existence of the related optimization problem.

## 4.1 Existence of the solutions to the optimization problem

If we use the standard five-point stencil ($n_s = 5$), and solve the constrained optimization problem (3.20)-(3.21) with equality constraints (3.27), we will get a first order method as we will prove later in this section. We first prove the existence of the solution to the optimization problem for the first order method. The stencil at an irregular grid point $(x_i, y_j)$ is composed of

$$(i-1,j),(i,j),(i+1,j),(i,j-1),(i,j+1) \tag{4.29}$$

corresponding to the index $k = 1, 2, 3, 4, 5$. For simplicity, we assume that $\beta$ is piecewise constant

$$\beta(x,y) = \begin{cases} \beta^+ & \text{if } (x,y) \in \Omega^+ \\ \beta^- & \text{if } (x,y) \in \Omega^-, \end{cases} \tag{4.30}$$

and $\kappa = 0$. We also assume that $h_x = h_y = h$. Under these assumptions, we can eliminate $\gamma_2$ from the first equation in (3.27) to get

$$\gamma_2 = -\sum_{k=1,k\neq 2}^{5} \gamma_k. \tag{4.31}$$

The equality and inequality constraints of the optimization problem are the following

$$\sum_{k=1,k\neq 2}^{5} \left(\frac{\xi_k}{\beta_k} - \frac{\xi_2}{\beta_k}\right) \gamma_k = 0, \tag{4.32}$$

$$\sum_{k=1,k\neq 2}^{5} (\eta_k - \eta_2)\, \gamma_k = 0, \tag{4.33}$$

$$\gamma_k \geq 0, \quad k = 1, 3, 4, 5, \tag{4.34}$$

where $\beta_k = \beta(x_{i+i_k}, y_{j+j_k})$ takes either $\beta^+$ or $\beta^-$ depending on which side of the interface the grid point $(x_{i+i_k}, y_{j+j_k})$ is. We will prove the following theorem.

**Theorem 4.1** *Let $(x_i^*, y_j^*)$ be a point on a piecewise smooth interface $\Gamma$ that satisfies*

$$|x_i^* - x_i| + |y_j^* - y_j| < 1. \tag{4.35}$$

*Assume that the interface $\Gamma$ cuts through the axes at no more than two points, and the tangent line at $(x_i^*, y_j^*)$ separates the grid points in the five-point stencil in the same way as the interface does. Then there is at least one set of solutions $\gamma_k > 0, k = 1, 3, 4, 5$ that satisfies (4.32)-(4.33).*

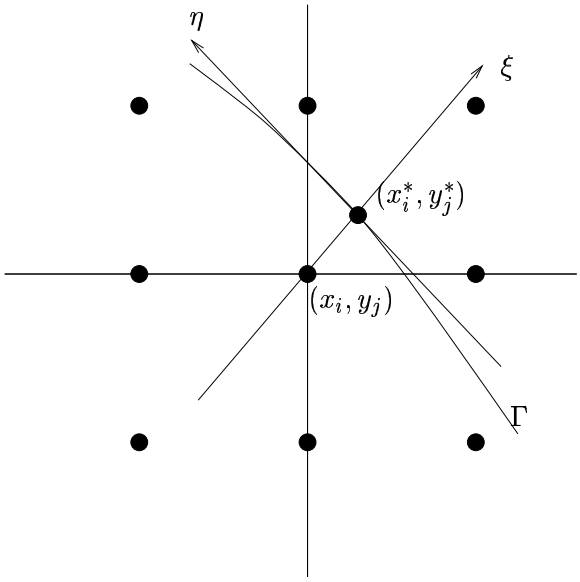


Figure 3: A diagram of the geometry at an irregular grid point if $h$ is sufficient small.

**Proof:** Without loss of generality, and for simplicity for indexing, we assume that $x_i^* - x_i \geq 0$, $y_j^* - y_j \geq 0$, the angle between the $x$- axis and the normal direction $\theta$ is in the interval $[0, \pi/2)$. There are two different cases depending on which side the grid point $(x_i, y_{j+1})$ is. We will prove one of cases as shown in Fig. 3. The proof of the other case is long and technically similar, so it will be omitted here. From Fig. 3, it is easy to see

$$\begin{aligned} &\xi_1 < 0, \quad \xi_3 > 0, \quad \xi_4 \leq 0, \quad \xi_5 \geq 0, \\ &\eta_1 \geq 0, \quad \eta_2 \leq 0, \quad \eta_4 < 0, \quad \eta_5 > 0. \end{aligned}$$

With such a geometry, the two equations (4.32) and (4.33) are

$$\left(\frac{\xi_1}{\beta^-} - \frac{\xi_2}{\beta^-}\right)\gamma_1 + \left(\frac{\xi_3}{\beta^+} - \frac{\xi_2}{\beta^-}\right)\gamma_3 + \left(\frac{\xi_4}{\beta^-} - \frac{\xi_2}{\beta^-}\right)\gamma_4 + \left(\frac{\xi_5}{\beta^+} - \frac{\xi_2}{\beta^-}\right)\gamma_5 = 0 \tag{4.36}$$

$$(\eta_1 - \eta_2)\,\gamma_1 + (\eta_3 - \eta_2)\,\gamma_3 + (\eta_4 - \eta_2)\,\gamma_4 + (\eta_5 - \eta_2)\,\gamma_5 = 0. \tag{4.37}$$

Introduce the parameters $a_{ij}$ as in the following

$$\begin{aligned} a_{11} &= -\left(\frac{\xi_1}{\beta^-} - \frac{\xi_2}{\beta^-}\right) > 0, \quad a_{13} = \frac{\xi_3}{\beta^+} - \frac{\xi_2}{\beta^-} > 0, \\ a_{14} &= -\left(\frac{\xi_4}{\beta^-} - \frac{\xi_2}{\beta^-}\right) \geq 0, \quad a_{15} = \frac{\xi_5}{\beta^+} - \frac{\xi_2}{\beta^-} \geq 0, \\ a_{23} &= -(\eta_3 - \eta_2) \geq 0, \quad a_{21} = (\eta_1 - \eta_2) \geq 0, \\ a_{24} &= -(\eta_4 - \eta_2) > 0, \quad a_{25} = (\eta_5 - \eta_2) > 0. \end{aligned}$$

We can rewrite the equations (4.36)-(4.37) as[2]

$$a_{13}\gamma_3 - a_{11}\gamma_1 = a_{14}\gamma_4 - a_{15}\gamma_5, \tag{4.38}$$

$$a_{23}\gamma_3 - a_{21}\gamma_1 = -a_{24}\gamma_4 + a_{25}\gamma_5. \tag{4.39}$$

We are ready to prove the theorem by distinguishing the following cases.

- $a_{23} = 0$. In this case, we also have $a_{21} = 0$. We choose

$$\gamma_5 = \frac{\beta_{i,j+1}}{h^2} > 0, \qquad \gamma_4 = \frac{a_{25}}{a_{24}}\gamma_5 > 0,$$
$$\gamma_1 = \frac{2\beta_{i-1,j}}{h^2} + \frac{|\, a_{14}\gamma_4 - a_{15}\gamma_5\,|}{a_{11}} > 0, \qquad \gamma_3 = \frac{1}{a_{13}}\left(a_{11}\gamma_1 + a_{14}\gamma_4 - a_{15}\gamma_5\right) > 0.$$

- $a_{14} = 0$. In this case, we also have $a_{15} = 0$. We choose

$$\gamma_1 = \frac{\beta_{i-1,j}}{h^2} > 0, \qquad \gamma_3 = \frac{a_{11}}{a_{13}}\gamma_1 > 0,$$
$$\gamma_4 = \frac{2\beta_{i,j-1}}{h^2} + \frac{|\, a_{23}\gamma_3 - a_{21}\gamma_1\,|}{a_{24}} > 0, \qquad \gamma_5 = \frac{1}{a_{25}}\left(a_{24}\gamma_4 + a_{23}\gamma_3 - a_{21}\gamma_1\right) > 0.$$

- $\dfrac{a_{11}}{a_{21}} = \dfrac{a_{13}}{a_{23}} = \tau > 0$. We choose

$$\gamma_4 = \frac{\beta_{i,j-1}}{h^2} > 0, \qquad \gamma_5 = \frac{a_{14} + \tau a_{24}}{a_{15} + \tau a_{25}}\gamma_4.$$

  With such choice of $\gamma_4$ and $\gamma_5$, we have

$$a_{14}\gamma_4 - a_{15}\gamma_5 = -\tau a_{24}\gamma_4 + \tau a_{25}\gamma_5.$$

  Then we choose

$$\gamma_1 = \frac{2\beta_{i,j-1}}{h^2} + \frac{|\, a_{14}\gamma_4 - a_{15}\gamma_5|}{a_{11}}$$
$$\gamma_3 = \frac{1}{a_{13}}\left(a_{11}\gamma_1 + a_{14}\gamma_4 - a_{15}\gamma_5\right).$$

- $\dfrac{a_{11}}{a_{13}} > \dfrac{a_{21}}{a_{23}}$. This is one of general cases. Consider the following two functions

$$g_1(\gamma_4, \gamma_5) = a_{14}\gamma_4 - a_{15}\gamma_5$$
$$g_2(\gamma_4, \gamma_5) = -a_{24}\gamma_4 + a_{25}\gamma_5.$$

  In the first quadrant of the $\gamma_4$-$\gamma_5$ plane, there are three different regions where $g_1 > g_2$, $g_1 = g_2$, and $g_1 < g_2$ respectively. Choose a point $\gamma_4^* > 0$, $\gamma_5^* > 0$ in the first quadrant of the $\gamma_4$, $\gamma_5$ plane in such a way that $g_1 < g_2$. Let $\gamma_1^*$, $\gamma_2^*$ be the solution to the system of equations (4.38)-(4.39) with $\gamma_4$-$\gamma_5$ being substituted by $\gamma_4^*$ and $\gamma_5^*$, since $\frac{a_{11}}{a_{13}} > \frac{a_{21}}{a_{23}}$, we can conclude that $\gamma_1^* > 0$ and $\gamma_2^* > 0$.

[2] It is also easy to show that $a_{23} = a_{21}$ and $a_{24} = a_{25}$.

- $\frac{a_{11}}{a_{13}} < \frac{a_{21}}{a_{23}}$. The proof is almost exactly the same as the previous case except we choose $\gamma_4^* > 0$, $\gamma_5^* > 0$ such that $g_1 > g_2$.

**Remark 4.1** *If the interface is smooth, then the conditions in Theorem 4.1 will be satisfied if $h$ is small enough. For a coarse grid, occasionally, the conditions in Theorem 4.1 may be violated. Some modification may be needed. In practice, we do not need to check the conditions in Theorem 4.1. Most of quadratic optimization solvers will either return an error indicator or wrong solution in such cases. We then can decide to take an alternative scheme at these grid points. Note that compared with the ghost fluid method, the methods proposed here do not need to move interface and decompose the flux jump condition.*

**Corollary 4.1** *From the proof of the existence of the optimization problem, we can conclude that*

$$|\gamma_k| \le \frac{C}{h^2}, \quad k = 1, 2, \cdots, 5,$$

*and there is at least one of $\gamma_k$ from each side of the interface such that*

$$|\gamma_k| \ge \frac{\bar{C}}{h^2},$$

*where the constants are $O(1)$ and independent of the grid points, but depend on the coefficient $\beta$.*

This corollary is useful in proving the convergence of the first order method.

## 4.2 Convergence proof of the first order method

We need the following lemma which is a generalization of Theorem 6.1 and Theorem 6.2 of Morton & Mayer's book [28] for multiple sub-regions $J_i$.

**Lemma 4.1** *Given a finite difference scheme $L_h$ defined on a discrete set of interior points $J_\Omega$ for Dirichlet elliptic equations, we assume the following conditions hold:*

1. *$J_\Omega$ can be partitioned into a number of disjoint regions*

$$J_\Omega = J_1 \cup J_2 \cup J_3 \cdots \cup J_s, \quad J_i \cap J_k = \emptyset, \quad \text{if } i \ne k. \tag{4.40}$$

2. *The truncation error of the finite difference scheme at a grid point $p$ satisfies*

$$|T_p| \le T_i, \quad \forall p \in J_i, \quad i = 1, 2, \cdots, s. \tag{4.41}$$

3. *There exists a non-negative mesh function $\phi$ defined on $\cup_{i=1}^s J_i$ satisfying*

$$L_h \phi_p \ge C_i > 0, \quad \forall p \in J_i, \quad i = 1, 2, \cdots, s. \tag{4.42}$$

*Then the global error of the approximate solution from the finite difference scheme at mesh points is bounded by*

$$||E_h||_\infty \leq \left( \max_{A \in J_{\partial\Omega}} \phi_A \right) \max_{1 \leq i \leq s} \left\{ \frac{T_i}{C_i} \right\}, \tag{4.43}$$

*where $E_h$ is the difference of the exact solution of the differential equation and the approximate solution of the finite difference equations at the mesh points, and $J_{\partial\Omega}$ is the set that contains the boundary points.*

**Theorem 4.2** *Let $u(x, y)$ be the exact solution to (1.1) and (1.2) with $\kappa = 0$, piecewise $\beta$ as defined in (4.30), and a Dirichlet boundary condition. Assume*

1. *the optimization problem (3.20)-(3.21) has a set of solution $\gamma_k$ with the first three equations in (3.17) being satisfied exactly or to the leading order at every irregular grid points;*
2. *$u(x, y)$ has piecewise continuous second order derivatives;*
3. *$h$ is sufficient small;*
4. *at all irregular grid points, the following is true:*

$$\sum_{\xi_k \geq 0} \gamma_k \xi_k \geq \frac{C_1}{h}. \tag{4.44}$$

*Then we have the following error estimate for the approximate solution obtained from the first order optimization method*

$$\|u(x_i, y_j) - U_{ij}\|_\infty \leq Ch, \tag{4.45}$$

*where $C = O(1)$ depends on the geometry, the coefficient $\beta$.*

**Proof:** If $h$ is sufficient small, we have proved that the optimization problem has solutions. Consider the solution to the following interface problem

$$\begin{aligned} \nabla \cdot \beta \nabla \phi &= 1, \\ [\phi] = 0, \qquad & [\beta \phi_n] = 1, \quad \phi_{\partial\Omega} = 1. \end{aligned} \tag{4.46}$$

From the results in [2, 6], we know that the solution $\phi$ exists, unique, and piecewise continuous. Therefore the solution is also bounded. In fact, with piecewise $\beta$, we can further prove that the solution is also piecewise smooth using integral equations, see the Appendix. Let

$$\bar{\phi}(x, y) = \phi(x, y) + \left| \min_{(x,y) \in \Omega} \phi(x, y) \right|. \tag{4.47}$$

Then $\bar{\phi}(x, y) \geq 0$ and still satisfy the differential equation and the jump conditions in (4.46). We define the discrete finite difference operator as

$$L_h u(x_i, y_j) = \sum_k^{n_s} \gamma_k \, u(x_{i+i_k}, y_{j+j_k}). \tag{4.48}$$

Let $(x_i, y_j)$ be an irregular grid point. If $h$ is small enough, then we know that $\gamma_k$ is bounded by $C/h^2$. Therefore we have

$$\begin{aligned} L_h\bar{\phi}(x_i,y_j) &= \sum_k^{n_s} \gamma_k\, \bar{\phi}(x_{i+i_k}, y_{j+j_k}) \\ &= (a_1+a_2)\bar{\phi}^- + \left(a_3 + \rho a_4 - a_8\frac{[\beta]\chi''}{\beta^+}\right)\bar{\phi}_\xi^- + \\ &\quad + \left(a_5 + a_6 - a_8\frac{[\beta_\eta]}{\beta^+} + a_{12}(1-\rho)\,\chi''\right)\bar{\phi}_\eta^- + \sum_{\xi_k\geq 0}\gamma_k\xi_k + O(1) \\ &= \sum_{\xi_k\geq 0}\gamma_k\xi_k + O(1), \end{aligned}$$

where $a_k$ are defined in (3.14). Note that $a_8\beta\chi''/\beta$, $a_8\beta_\eta/\beta$, and $a_{12}(1-\rho)\,\chi''$ are $O(1)$ terms. The condition $\gamma_k \leq C/h^2$ is needed to guarantee that the lower order term is $O(1)$ but not larger. Thus from (4.44), the comparison function $\bar{\phi}$ satisfies

$$L_h\bar{\phi}(x_i,y_j) = \begin{cases} 1 + O(h^2) & \text{if } (x_i,y_j) \text{ is a regular grid point,} \\ \displaystyle\sum_{\xi_k\geq 0}\gamma_k\xi_k \geq \frac{C_1}{h} + O(1) & \text{if } (x_i,y_j) \text{ is an irregular grid point.} \end{cases}$$

At *a regular* grid points we have

$$\frac{|T_{ij}|}{L_h\bar{\phi}(x_i,y_j)} \leq \frac{C_2h^2}{1} = C_2h^2. \tag{4.49}$$

At an irregular grid points we have

$$\frac{|T_{ij}|}{L_h\bar{\phi}(x_i,y_j)} \leq \frac{C_3}{C_1/h} = \frac{C_3}{C_1}h. \tag{4.50}$$

From Lemma 4.1, we conclude the global error then satisfies

$$\|u(x_i,y_j) - U_{ij}\|_\infty \leq \left(\max_{(x,y)\in\partial\Omega}\phi(x,y)\right)\max\left\{\frac{C_3}{C_1}, C_2h\right\}h \tag{4.51}$$

$$\leq Ch. \tag{4.52}$$

**Remark 4.2** *1. The term $\sum_{\xi_k\geq 0}\gamma_k\xi_k$ acts as a discrete delta function to the singular source in the following equation*

$$\nabla\cdot(\beta\nabla u) = \int_\Gamma \delta_2(\mathbf{x} - X(s))ds.$$

*Thus generally we can expect $\sum_{\xi_k\geq 0}\gamma_k\xi_k$ to be $O(1/h)$ since $\gamma_k$ is $O(1/h^2)$, except when all the grid points from other side of the interface other than $(x_i,y_j)$ are very close to the interface. In this case, the finite difference scheme usually turns out to be close to the standard central finite difference scheme with the correction term mainly involves the jump in the solution.*

2. *First order convergence also seems to be obvious with the following common belief: the approximation at the boundary can be one order lower than that in the interior domain without affecting global order accuracy. Since the interface is an internal boundary with local truncation error being $O(1)$, we can expect the global error to be $O(h)$. For one-dimensional elliptic equations, this has been quantitatively explained in [4] which we briefly explain below for our problem. Since the problem is linear, the error $E_{ij} = u(x_i, y_j) - U_{ij}$ should satisfy the finite difference equation with a discrete source term*

$$F_{ij} = \begin{cases} 0 & \text{at a regular grid point and the boundary,} \\ h\dfrac{C_{ij}}{h} & \text{at an irregular grid point,} \end{cases}$$

*if we neglect high order terms. An irregular grid point $(x_i, y_j)$ is near the interface, thus the leading error term $C_{ij} = O(1)$ is a quantity that is defined on the interface. Therefore $E_{ij}$ can be regarded as a discrete solution to the continuous problem*

$$\begin{aligned} \nabla \cdot (\beta \nabla e) &= h \int_\Gamma C(s)\delta_2(\mathbf{x} - X(s))ds, \\ e|_{\partial\Omega} &= 0, \end{aligned}$$

*for some function $C(s)$ defined along the interface. This boundary value problem has a bounded solution of $O(\|C\|_{L^\infty(\Gamma)}h)$ and thus we conclude that $E_{ij} = \bar{C}h$.*

# 5 Convergence of the second order methods

In general we may argue that if we enclose enough grid points, then the six equations (3.17) and the sign property are satisfied and in turn we obtain a second order method. As we discussed in Section 3, we use the standard nine-point stencil and prove indeed that our claim holds. First, we will show numerically below that the corresponding optimization problems have solutions that are bounded.

## 5.1 Numerical proof of the existence of the solution to the optimization problem.

We again assume that $\kappa = 0$ in (1.1), and the $h$ is small enough that the interface behaviors like a straight line relative to the underlying grid. We also assume that $\beta$ is piecewise constant as in (4.30). Under these conditions, the coefficients of the system of equations that contain $\chi''$ in the second and the third equations of (3.17) are high order term $O(h^2)$ compared to those in $a_3$ and $\rho a_4$ which are $O(h)$. We will neglect these high order terms $O(h^2)$. In other words, if $h$ is sufficient small, the existence of the solution to the optimization problem is independent of the curvature of the interface, assuming that the Kuhn-Tucker condition for the binding constraints is satisfied. With the standard nine-point stencil, we will numerically prove the following theorem.

**Theorem 5.1** *Let $(x_i, y_j)$ be an irregular grid point, and $(x_i^*, y_j^*)$ be its projection on the interface, Then the optimization problem defined in (3.20)-(3.21) with six equality and the sign constraints*

*has solutions. The solution of the coefficients $\gamma_k$ also satisfy*

$$\left|\frac{\gamma_k}{\beta^-}\right| \le \frac{C}{h^2}, \quad k = 1, \cdots, 9. \tag{5.53}$$

*Furthermore there are $\gamma_k$'s from each side of the interface such that*

$$\left|\frac{\gamma_k}{\beta^-}\right| \ge \frac{C_1}{h^2}, \tag{5.54}$$

*and*

$$\sum_{\xi_k \ge 0} \gamma_k \xi_k \ge \frac{C_2}{h}, \quad \textit{if} \quad \max_{\xi_k \ge 0} \{\, \xi_k \} \ge C_3\, h. \tag{5.55}$$

*The constants are $O(1)$ which depend on the coefficient $\beta$ but are independent of $i$ and $j$.*

**Proof:** Take a typical irregular grid points $(x_i, y_j)$. First we can shift and scale the problem in the following way:

$$\bar{x} = \frac{x - x_i}{h}, \quad \bar{y} = \frac{y - y_j}{h}, \quad \bar{\gamma}_k = \frac{\gamma_k}{h^2}.$$

For simplicity, we will use the same notations without bars. The nine-point stencil then is the square $-1 \le x, y \le 1$. With the local coordinates, we can just consider the case that the projection is in the first quadrant.

Given any point $(x^*, y^*)$, and an angle $\theta$

$$0 \le x^* \le 1, \qquad 0 \le y^* \le 1 - x^*, \qquad 0 \le \theta \le \frac{\pi}{2}, \tag{5.56}$$

we can write down the equation of the interface as

$$\cos\theta\,(x - x^*) + \sin\theta\,(y - y^*) = 0. \tag{5.57}$$

The interface will cut the square $-1 \le x, y \le 1$ into two parts. We denote the side which contains the origin as $-$ side, and the other one as $+$ side. We also scale the coefficient $\beta$ either as $\beta^- = 1$, $\beta^+ = 1/\rho$, or $\beta^+ = 1$, $\beta^- = \rho$.

The optimization problem is:

$$\begin{aligned} & \min_{\gamma} \frac{1}{2} \sum_k (\gamma_k - g_k)^2 \\ s.t. \quad & A\gamma = b, \quad \gamma_k \ge 0, \quad \text{if} \quad (i_k, j_k) \ne (0,0) \quad \gamma_k < 0, \quad \text{if} \quad (i_k, j_k) = (0,0), \end{aligned}$$

where

$$\begin{aligned} g_k &= \beta^{\pm}, \quad (i_k, j_k) \in \{(-1,0), (1,0), (0,-1), (0,1)\ \}, \\ g_k &= -4, \quad (i_k, j_k) = (0,0), \\ g_k &= 0, \quad \text{Otherwise}, \end{aligned}$$

and $A\gamma = b$ is the following system of equations:

$$\begin{aligned} a_1 + a_2 &= 0 \\ a_3 + \rho a_4 &= 0 \\ a_5 + a_6 &= 0 \\ a_7 + a_8\,\rho &= \beta^- \\ a_9 + a_{10} + a_8\,(\rho - 1) &= \beta^- \\ a_{11} + a_{12}\,\rho &= 0. \end{aligned}$$

To solve the problem numerically, we use a uniform grid

$$\begin{aligned} r_i &= i\,\Delta r, \quad \Delta r = \frac{1}{m}, \quad i = 0, 1, \cdots, m, \\ \theta_j &= j\,\Delta\theta, \quad \Delta\theta = \frac{\pi}{2n}, \quad j = 0, 1, \cdots, n, \\ \rho_k &= 10^{-N_1 + k\,\Delta\rho}, \quad \Delta\rho = \frac{N_2 + N_1}{L}, \quad k = 0, 1, \cdots, L. \end{aligned}$$

The projection then is determined by

$$x_i^* = r_i\,\cos\theta_j, \quad y_i^* = r_i\,\sin\theta_j$$

excluding those $y_i^* > 1 - x_i^*$ that are outside of the five-point stencil. Define

$$\begin{aligned} \gamma_{max}(\rho) &= \max_{r_i,\theta_j} \max_{1\le k\le 9} \frac{|\gamma_k|}{\beta^-} = \max_{r_i,\theta_j} \frac{|\gamma_5|}{\beta^-} \\ \gamma_{min}(\rho) &= \min_{r_i,\theta_j} \frac{|\gamma_5|}{\beta^-} \\ S_{min}(\rho) &= \min_{r_i,\theta_j,\max_{\xi_k\ge 0}\{\xi_k\}\ge C_3 h} \sum_{\xi_k \ge 0} \xi_k \gamma_k. \end{aligned}$$

Our numerical tests show that the solution to the optimization problem always exits. Figure 4 and Figure 5 summarize the numerical proof about the magnitude of the finite difference coefficients. In Figure 4, the dashed line is $\gamma_{max}(\rho)$ and it is bounded by $|\gamma_k|\,h^2 \le 10$. The solid line is $\gamma_{min}(\rho)$ and $|\gamma_5|\,h^2 \ge 1$. If $\beta^- = \beta^+$, we will have $\gamma_5 h^2 = 4$ exactly as we can see from Figure 4. Therefore Figure 4 confirms the inequalities (5.53) and (5.54).

In Figure 4, we plot $hS_{min}(\rho)/C_2$ where

$$C_2 = \frac{\max\{\beta^-/\beta^+, \beta^-/\beta^+\}}{\max\{1,\,\beta^-\}\ \max\{1,\,\beta^+\}}. \tag{5.58}$$

This constant was found by numerical experiments. The minimum of $\sum_{\xi_k\ge 0} \gamma_k \xi_k$ is taken all cases except for two points $(1, 0)$ and $(0, 1)$ where the interface actually is $x = 1$ and $y = 1$ respectively. In these cases, the grid points touch the interface and the finite difference scheme is the standard five-point stencil scheme with possible non-zero correction $C_{ij}$ for the jump in the solution and the flux. In Figure 4 (a) and Figure 4 (b), we always have

$$\sum_{\xi_k \ge 0} \gamma_k \xi_k \ge \frac{0.01\,C_2}{h}, \quad \text{if} \quad \sum_{\xi_k \ge 0} \{\xi_k\} \ge C_3 h.$$

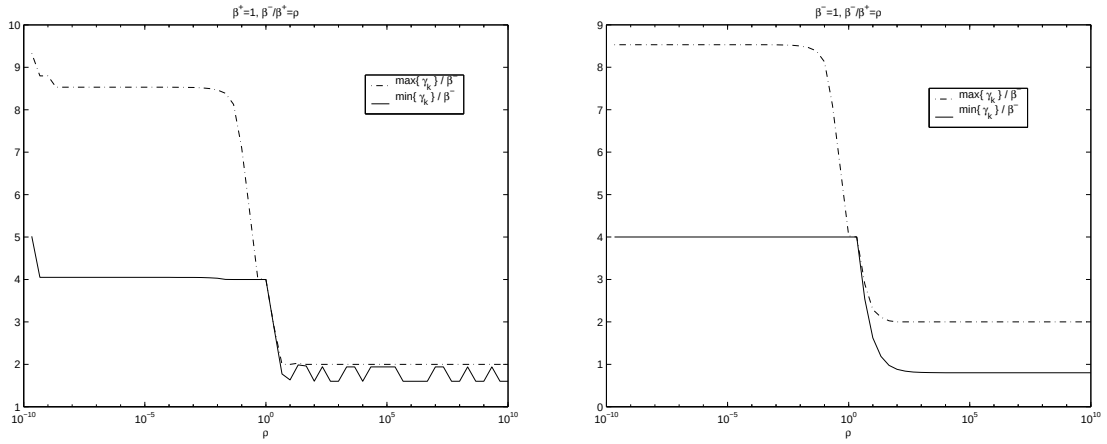


Figure 4: The computed $\gamma_{max}(\rho)$ and $\gamma_{min}(\rho)$ with $m = n = L = 60$, $N_1 = 9$, and $N_2 = 10$. (a) $\beta^- = 1$, $\beta^+ = 1/\rho$. (b) $\beta^+ = 1$, $\beta^- = \rho$.

Thus the numerical proof confirms the inequality (5.55). We have tried different grids size and all the results showed the same results. Even though we can not test all possible $\beta$, the jump in the ratio is large enough (from $10^{-9}$ to $10^{10}$) that should cover most of applications.

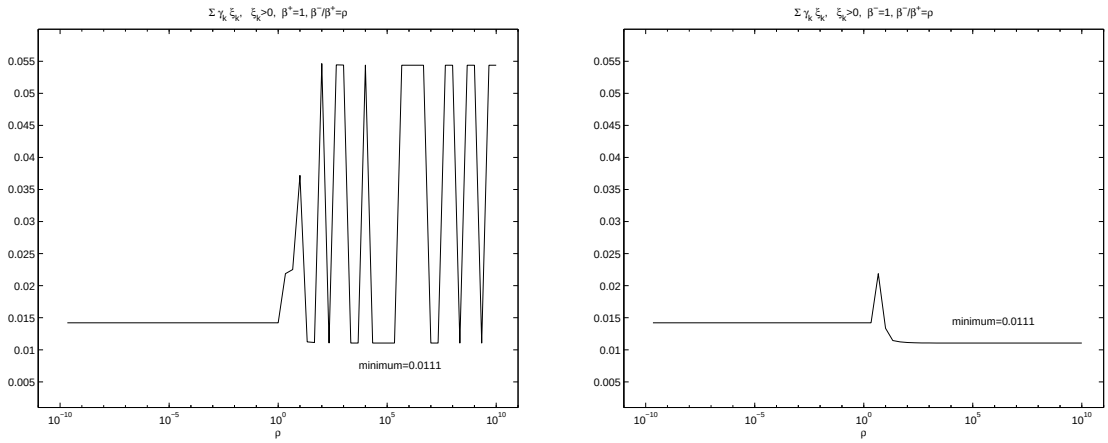


Figure 5: The computed $S_{min}(\rho)$ with $m = n = L = 60$, $N_1 = 9$, and $N_2 = 10$. (a) $\beta^- = 1$, $\beta^+ = 1/\rho$. (b) $\beta^+ = 1$, $\beta^- = \rho$.

The complete theoretical proof of the theorem is difficult. However we have proved (5.53) in the theorem for the case $\rho \geq 1$ assuming the optimization problem has solutions.

**Theoretical Proof of (5.53) when $\rho \geq 1$:** We assume that the optimization problem has solutions and $\beta^- \geq \beta^+$. Since $(x_i^*, y_j^*)$ is the projection of $(x_i, y_j)$ on the interface, we know that $\eta_{k_c} = 0$, where $k_c$ is the $k$ such that $(i_{k_c}, j_{k_c}) = (0, 0)$. From the fifth equation in (3.17)

$$\sum_{k=1}^{n_s} \gamma_k \frac{\eta_k^2}{2} + a_8(\rho - 1) = \beta^-,$$

and the fact that $a_8 \geq 0$ and $\rho \geq 1$, we can conclude that

$$\sum_{k=1}^{n_s} \gamma_k \frac{\eta_k^2}{2} \leq \beta^-,$$

and $\gamma_k \leq C/h^2$ except at most two possible $k$, say $k_1,\ k_2$ where $\eta_k$ is very small, see Fig. 3 for an illustration. The possible such $k$'s in Fig. 3 are $k = 1$ and $k = 9$ corresponding to the grid points $(x_{i-1}, y_{j-1})$ and $(x_{i+1}, y_{j+1})$. Note that $(x_{i_{k_1}}, y_{j_{k_1}})$ and $(x_{i_{k_2}}, y_{j_{k_2}})$ have to be on different sides of the interface. Without loss of generality, we assume that $\xi_{k_1} \leq 0$ and $\xi_{k_2} \geq 0$. From the second equation and the fourth equations in (3.17) we have

$$\gamma_{k_1}\left(\frac{h\xi_{k_1}}{\beta^-} - \frac{h\xi_{k_c}}{\beta^-}\right) + \gamma_{k_2}\left(\frac{h\xi_{k_2}}{\beta^+} - \frac{h\xi_{k_c}}{\beta^-}\right) \approx O(1),$$

$$\gamma_{k_1}\left(\frac{\xi_{k_1}^2}{\beta^-} - \frac{\xi_{k_c}^2}{\beta^-}\right) + \gamma_{k_2}\left(\frac{\xi_{k_2}^2}{\beta^+} - \frac{\xi_{k_c}^2}{\beta^-}\right) \approx O(1).$$

The determinant $J$ of the $2 \times 2$ matrix of the system of equations above is given by

$$J = h\frac{\xi_{k_1} - \xi_{k_c}}{\beta^-}\left((\frac{\xi_{k_2}^2}{\beta^+} - \frac{\xi_{k_c}^2}{\beta^-}) - (\xi_{k_1} + \xi_{k_c})(\frac{h\xi_{k_2}}{\beta^+} - \frac{h\xi_{k_c}}{\beta^-})\right).$$

Since $\xi_{k_1} \leq -h \leq \xi_{k_c} < 0$, $\xi_{k_2} > 0$, there exists a constant $c_1 > 0$ such that

$$(\frac{\xi_{k_2}^2}{\beta^+} - \frac{\xi_{k_c}^2}{\beta^-}) - (\xi_{k_1} + \xi_{k_c})(\frac{\xi_{k_2}}{\beta^+} - \frac{\xi_{k_c}}{\beta^-}) = \frac{\xi_{k_2}^2}{\beta^+} - (\xi_{k_1} + \xi_{k_c})\frac{\xi_{k_2}}{\beta^+} + \xi_{k_1}\frac{\xi_{k_c}}{\beta^-} \geq c_1 h^2.$$

Since $\xi_{k_1} - \xi_{k_c} \leq -c_2 h$ for some $c_2 > 0$, it follows that $J \leq -ch^4$ for some $c > 0$ and thus we have $\gamma_{k_1},\ \gamma_{k_2} \leq c/h^2$. $\square$

Similarly, for the case $\rho \leq 1$ if $a_7 \geq 0$ then (5.53) holds. In fact, from the forth and fifth equations of (3.17)

$$a_7 + a_8 = a_9 + a_{10}$$

Since $a_7 \geq 0$ it follows from the forth equation of (3.17) that

$$a_7 + a_8 = a_9 + a_{10} \leq \beta^+.$$

Thus exactly the same argument as above is applied.

## 5.2 Convergence of the second order method.

Parallel to the convergence result for the first order method, we have the following theorem:

**Theorem 5.2** *Let $u(x, y)$ be the exact solution to (1.1) and (1.2) with $\kappa = 0$, piecewise $\beta$ as defined in (4.30), and a Dirichlet boundary condition. Assume*

1. *the optimization problem (3.20)-(3.21) has a set of solution $\gamma_k$ with all the six equations in (3.17) being satisfied at every irregular grid points;*

2. *$u(x,y)$ has piecewise continuous fourth order derivatives;*

3. *$h$ is sufficient small;*

4. *at all irregular grid points, the following is true:*

$$\sum_{\xi_k \geq 0} \gamma_k \xi_k \geq \frac{C_1}{h}, \tag{5.59}$$

*or*

$$\max_{\xi_k \geq 0} \{\xi_k\} \leq C_2 h \quad \textit{with } C_2 > 0 \textit{ sufficiently small.} \tag{5.60}$$

*Then we have the following error estimate for the approximate solution obtained from the first order optimization method*

$$\|u(x_i, y_j) - U_{ij}\|_\infty \leq C_3 h^2, \tag{5.61}$$

*where the constants depend on the geometry and the coefficient $\beta$.*

**Remark:** We have numerically proved that (5.59) holds as long as $\max_{\xi_k \geq 0} \{\xi_k\} > C_2 h$ with $C_2 = 0.01$. Otherwise (5.59) may not hold. However, we will show that quadratic convergence can still be proved by constructing a modified comparison function in the following proof.

**Proof:** If (5.59) is true, then we know that

$$L_h \bar{\phi}(x_i, y_j) = \sum_{\xi_k \geq 0} \gamma_k \xi_k + \text{lower order terms} \geq \frac{C_1}{h},$$

where $\bar{\phi}(x,y)$ is defined in (4.47) in Section 4. If (5.59) is violated but (5.60) is true, then all the grid points from other side of the interface other than $(x_i, y_j)$ are very close to the interface. For the nine-point stencil, this can only happen when the interface is very close to one of the grid lines, $x = x_{i-1}$, or $x = x_{i+1}$, or $y = y_{j-1}$, or $y = y_{j+1}$. Without loss of generality, we assume that the interface cuts the grid line $y = y_j$ at $x_i^*$, where

$$x_i < x_i^* \leq x_{i+1}, \qquad x_{i+1} - x_i^* \leq C_2 h.$$

The normal direction is nearly parallel to the $x$- axis. Since $\max_{\xi_k \geq 0} \{\xi_k\} \leq C_2 h$, we know that $(x_{i+1}, y_j)$, $(x_{i+1}, y_{j-1})$, and $(x_{i+1}, y_{j+1})$ are only three grid points in the nine-point stencil that are in the different side from $(x_i, y_j)$, and $(x_i^*, y_j)$ is very close to the projection of $(x_i, y_j)$ on the interface. Since there is no interface involved in the $y$ direction, we can decompose the equations (3.17) in the $x$- and $y$- directions. In the $y$- direction, assuming $(x_i, y_j)$ is in $-$ side, we have

$$\beta^- \frac{u(x_i, y_{j-1}) - 2u(x_i, y_j) + u(x_i, y_{j+1})}{h^2} = \beta^- u_{yy}(x_i, y_j) + O(h^2),$$

which is the standard three-point difference scheme.

In the $x$- direction, consider also the three-point difference scheme: The equations in the $x$-direction are

$$\begin{aligned} \tilde{a}_1 + \tilde{a}_2 &= 0, \\ \tilde{a}_3 + \rho \tilde{a}_4 &= 0, \\ \tilde{a}_7 + \tilde{a}_8 \rho &= \beta^-, \end{aligned}$$

where we use $\tilde{a}_i$ to represent those terms in $x$- directions in $a_i$'s in (3.17). From the one-dimensional result, see [18] we have that the solution to the equations above is also close to the standard three point central difference scheme for $u_{xx}(x_i, y_j)$ since $\tilde{a}_4/h$, $\tilde{a}_8/h^2$ are of order $O(C_2)$. From (3.20)-(3.21) of the constructed optimization problem, we can conclude that the solution to the optimization problem is close to the standard five-point stencil scheme with a correction term of $O(C_2/h^2)$. For such a point, we define a function

$$\psi_{ij}^x(x) = \begin{cases} \dfrac{(x_i^* - x_i)(x_i - x)}{\gamma_{ij}^{(2)} h^3}, & \text{if } x \le x_i^*, \\ \dfrac{(x_{i+1} - x_i^*)(x - x_{i+1})}{\gamma_{i+1,j}^{(8)} h^3}, & \text{if } x > x_i^*, \end{cases} \tag{5.62}$$

where $\gamma_{ij}^{(2)}$ is the coefficient of the finite difference scheme centered at $(x_i, y_j)$ corresponding to the grid point $(x_{i-1}, y_j)$ with $k = 2$; $\gamma_{i+1,j}^{(8)}$ is the coefficient of the finite difference scheme centered at $(x_{i+1}, y_j)$ corresponding to the grid point $(x_{i+2}, y_j)$ with $k = 8$. Notice that $\psi_{ij}^x(x_i) = \psi_{ij}^x(x_{i+1}) = 0$ and $\psi_{ij}^x(x_j) > 0$ for $j \neq i,\ i+1$ and that $\psi_{ij}^x(x) \le M$ for all $(x, y) \in \Omega$. More important, we can easily derive

$$L_h \psi_{ij}^x(x_i, y_j) = \frac{x_i^* - x_i}{h^2}(1 + O(C_2)), \tag{5.63}$$

$$L_h \psi_{ij}^x(x_{i+1}, y_j) = \frac{x_{i+1} - x_i^*}{h^2}(1 + O(C_2)). \tag{5.64}$$

The high order terms are due to the fact that $L_h$ may not be exact the standard five-point finite difference scheme although it is close. Therefore when all $\xi_k \ge 0$ is very small, $x_i^* - x_i$ is close to $h$ and $L_h \psi_{ij}^x(x_i, y_j) \ge 1/h$.

Similarly we can construct such $\psi_{ij}^x(x)$ or $\psi_{ij}^y(y)$ at the points where (5.60) holds. Define the comparison function as

$$\tilde{\phi}(x, y) = \bar{\phi}(x, y) + \sum \psi_{ij}^x(x) + \sum \psi_{ij}^y(y),$$

where $\bar{\phi}$ is the same as defined in (4.47) in Section 4. Then

$$L_h \tilde{\phi}(x_i, y_j) \ge \begin{cases} 1 + O(h^2) & \text{if } (x_i, y_j) \text{ is a regular grid point,} \\ \displaystyle\sum_{\xi_k \ge 0} \gamma_k \xi_k \ge \frac{C_1}{h} + O(1) & \text{if (5.59) is true.} \\ \dfrac{1 - C_2}{h} & \text{if } \max\limits_{\xi_k \ge 0} \{\xi_k\} \le C_2 h, \text{ with } C_2 \ll 1. \end{cases}$$

Note that at some regular grid points, $L_h \tilde{\phi}(x_i, y_j)$ can be very large but it is nonnegative. Thus, the first inequality above still holds. Therefore at a regular points we have

$$\frac{|T_{ij}|}{L_h \tilde{\phi}(x_i, y_j)} \le \frac{C_3 h^2}{1}.$$

At an irregular grid point where (5.59) is satisfied, we have

$$\frac{|T_{ij}|}{L_h \tilde{\phi}(x_i, y_j)} \le \frac{C_4 h}{C_1/h} = \frac{C_4}{C_1} h^2$$

since the truncation error is bounded by

$$|T_{ij}| \le C_4 h$$

for some constant $C_4$ that depends on the third derivatives of the solution on each side of the interface. At an irregular grid point where the (5.60) is true, we also have

$$\frac{|T_{ij}|}{L_h\tilde{\phi}(x_i,y_j)} \le \frac{C_4 h}{(1-C_2)/h} = \frac{C_4}{1-C_2}\,h^2.$$

Thus, from Lemma 4.1, again we have proved the quadratic convergence.

Notice that, if $h$ is small enough, we have numerically proved the existence of the solution to the optimization problems and (5.59) piecewise constant $\beta$, therefore the method using the standard nine-point stencil is second order convergent.

For ***variable coefficient*** $\beta$ ***and non zero jump*** $[\kappa]$, since all the terms in the linear system of equations (3.17) that involve $[\kappa]$ and the derivatives of $\beta$ are high order terms of $h$, we can conclude the same result if $h$ is sufficient small theoretically. Our numerical tests have verified second order accuracy for piece-wise and variable discontinuous coefficients through grid refinement analysis even if $h$ is relatively large.

# 6 Numerical Results

We have performed a number of number of numerical experiments for both first order and second order methods. The results agree with our theoretical analysis. The computation are done using either Sun's Ultra-1 workstation or IBM SP2 machine. The linear system of equations is solved using the multigrid method developed by P. M. de Zeeu [8]. MGD9V takes the standard nine point stencil. Our code is modified from the package developed in [18]. The interface is a closed curve in the solution domain and expressed in terms of the periodic cubic spline interpolation.

## 6.1 Grid refinement analysis

**Example 6.1**

This example is the same as the example 2 in [15]. The interface is the circle $x^2+y^2=\frac{1}{4}$ within the computation domain $-1 \le x, y \le 1$. The equations are

$$(\beta u_x)_x + (\beta u_y)_y = f(x,y) + C\int_\Gamma \delta(\vec{x}-\vec{X}(s))\,ds, \tag{6.65}$$

with $\quad f(x,y) = 8\,(x^2+y^2)+4 \qquad$ and

$$\beta(x,y) = \begin{cases} x^2+y^2+1, & \text{if } x^2+y^2 \le \frac{1}{4}, \\ b, & \text{if } x^2+y^2 > \frac{1}{4}. \end{cases}$$

Dirichlet boundary conditions are determined from the exact solution

$$u(x,y) = \begin{cases} r^2, & \text{if } r \le \frac{1}{2}, \\ (1-\frac{1}{8\,b}-\frac{1}{b})/4 + (\frac{r^4}{2}+r^2)/b + C\,\log(2r)/b, & \text{if } r > \frac{1}{2}. \end{cases} \tag{6.66}$$

(a) $b = 10,\ C = 0.1.$

| $n_{finest}$ | $n_1$ | level | $n_{coarse}$ | $\| E_n \|_\infty$ | order |
|---|---|---|---|---|---|
| 42 | 40 | 4 | 6 | $5.0184\ 10^{-3}$ | |
| 82 | 80 | 5 | 6 | $1.7610\ 10^{-3}$ | 1.5652 |
| 162 | 160 | 6 | 6 | $1.4726\ 10^{-3}$ | 0.2628 |
| 322 | 320 | 7 | 6 | $5.3827\ 10^{-4}$ | 1.4650 |
| 642 | 640 | 8 | 6 | $2.6156\ 10^{-4}$ | 1.0459 |

(b) $b = 0.1,\ C = 0.1.$

| $n_{finest}$ | $n_1$ | level | $n_{coarse}$ | $\| E_n \|_\infty$ | order |
|---|---|---|---|---|---|
| 42 | 40 | 4 | 6 | $3.8393\ 10^{-1}$ | |
| 82 | 80 | 5 | 6 | $1.2884\ 10^{-1}$ | 1.6320 |
| 162 | 160 | 6 | 6 | $9.7770\ 10^{-2}$ | 0.4053 |
| 322 | 320 | 7 | 6 | $3.7634\ 10^{-2}$ | 1.3898 |
| 642 | 640 | 8 | 6 | $1.8031\ 10^{-2}$ | 1.0663 |

Table 1: Numerical results of the first order method for Example 6.1. First order convergence is observed.

It is easy to check that (6.66) satisfies (6.65). In this example, we have variable and discontinuous coefficients. Table 1 and Table 2 give numerical results using the first order method and the second order method for different choices of $b$ and $c$. The maximum error over all grid points,

$$\| E_n \|_\infty = \max_{i,j} \mid u(x_i, y_j) - U_{ij} \mid,$$

is presented, where $U_{ij}$ is the computed approximation at the uniform grid points $(x_i, y_j)$. The order of convergence is computed from

$$\text{order} = \left| \frac{\log (\| E_{n_1} \|_\infty / \| E_{n_2} \|_\infty)}{\log(n_1/n_2)} \right|,$$

which is the solution of

$$\| E_n \|_\infty = C\, h^{\text{order}}$$

with two different $n$'s.

As explained earlier and in [20], for interface problems, the errors usually do not decline monotonously. Instead it depends on the relative location of the grid and the interface. However, we can easily observe the first order and second order convergence in Table 1 and Table 2. Notice that as the parameter $b$ gets smaller, the solution in the outside of the interface becomes larger and the problem becomes harder to solve. But our second order method still converges quadratically.

**Example 6.2**

In this example, the interface is the ellipse $x^2 + 4y^2 = 1$ within the computational domain $-2 \le x, y \le 2$. The equation is

$$\beta\,(u_{xx} + u_{yy}) = f(x, y),$$

(a) $b = 10,\ C = 0.1.$

| $n_{finest}$ | $n_1$ | level | $n_{coarse}$ | $\| E_n \|_\infty$ | order |
|---|---|---|---|---|---|
| 34 | 40 | 3 | 9 | $1.0179\ 10^{-3}$ | |
| 66 | 80 | 4 | 9 | $1.9532\ 10^{-4}$ | 2.4889 |
| 130 | 160 | 5 | 9 | $5.3213\ 10^{-5}$ | 1.9183 |
| 258 | 320 | 6 | 9 | $1.2102\ 10^{-5}$ | 2.1605 |
| 514 | 640 | 7 | 9 | $3.0413\ 10^{-6}$ | 2.0038 |

(b) $b = 1000,\ C = 0.1.$

| $n_{finest}$ | $n_1$ | level | $n_{coarse}$ | $\| E_n \|_\infty$ | order |
|---|---|---|---|---|---|
| 34 | 40 | 3 | 9 | $5.1361\ 10^{-4}$ | |
| 66 | 80 | 4 | 9 | $8.2345\ 10^{-5}$ | 2.7598 |
| 130 | 160 | 5 | 9 | $1.8687\ 10^{-5}$ | 2.1878 |
| 258 | 320 | 6 | 9 | $4.0264\ 10^{-6}$ | 2.2394 |
| 514 | 640 | 7 | 9 | $9.430\ 10^{-7}$ | 2.1059 |

(c) $b = 0.001,\ C = 0.1.$

| $n_{finest}$ | $n_1$ | level | $n_{coarse}$ | $\| E_n \|_\infty$ | order |
|---|---|---|---|---|---|
| 34 | 40 | 3 | 9 | 9.3464 | |
| 66 | 80 | 4 | 9 | 2.0055 | 2.3204 |
| 130 | 160 | 5 | 9 | $5.8084\ 10^{-1}$ | 1.8280 |
| 258 | 320 | 6 | 9 | $1.3741\ 10^{-1}$ | 2.1031 |
| 514 | 640 | 7 | 9 | $3.5800\ 10^{-2}$ | 1.9514 |

Table 2: Numerical results of the second order method for Example 6.1, second order convergence is observed.

(a) $\beta^+ = 1,\ \beta^- = 1000$

| $n_{finest}$ | $n_1$ | level | $n_{coarse}$ | $\| E_n \|_\infty$ | order |
|---|---|---|---|---|---|
| 34 | 40 | 3 | 9 | $1.8322\ 10^{-1}$ | |
| 66 | 80 | 4 | 9 | $3.5224\ 10^{-3}$ | 5.9574 |
| 130 | 160 | 5 | 9 | $4.5814\ 10^{-5}$ | 3.0090 |
| 258 | 320 | 6 | 9 | $1.4240\ 10^{-5}$ | 1.7049 |
| 514 | 640 | 7 | 9 | $3.1501\ 10^{-6}$ | 2.1887 |

(b) $\beta^+ = 1000,\ \beta^- = 1$

| $n_{finest}$ | $n_1$ | level | $n_{coarse}$ | $\| E_n \|_\infty$ | order |
|---|---|---|---|---|---|
| 34 | 40 | 3 | 9 | $8.0733\ 10^{-3}$ | |
| 66 | 80 | 4 | 9 | $3.0371\ 10^{-3}$ | 1.4739 |
| 130 | 160 | 5 | 9 | $7.1981\ 10^{-4}$ | 2.1238 |
| 258 | 320 | 6 | 9 | $1.6876\ 10^{-4}$ | 2.1162 |
| 514 | 640 | 7 | 9 | $2.7407\ 10^{-5}$ | 2.6371 |

Table 3: Numerical results of the second order method for Example 6.2, second order convergence is observed.

where the coefficients are defined as

$$\beta = \begin{cases} \beta^-, & \text{if } x^2 + 4y^2 \le 1, \\ \beta^+, & \text{if } x^2 + 4y^2 > 1. \end{cases}$$

The jumps $[u]$ in the solution, $[\beta u_n]$ in the flux, and $[f]$ in the source term are chosen so that the following function is the exact solution:

$$u(x,y) = \begin{cases} x^2 - y^2, & \text{if } x^2 + 4y^2 \le 1, \\ \sin(x)\cos(y), & \text{if } x^2 + 4y^2 > 1. \end{cases} \tag{6.67}$$

Unlike Example 6.1, the solution in this example is *discontinuous* and independent the coefficients $\beta$. Table 3 shows the results of the grid refinement analysis using the second order method. Again we see clearly second order accuracy. Fig. 6 (a) plot the solution which is composed of two pieces. Fig. 6 (b) is the error plot of the computed solution. The error looks like piecewise smooth as well.

It is worth to point out that, compared with the original immersed interface method, the error distribution obtained from the new methods developed here behaves much better due to the facts that (1) the resulting linear system of equation is an M-matrix; (2) more grid points are involved.

**Example 6.3**

Finally we show an example with the same solution inside and outside of the interface as the example above but with more complicated interface:

$$\rho = \frac{1}{2} + 0.1\ \sin(5\theta), \quad 0 \le \theta \le 2\pi. \tag{6.68}$$

Fig. 7 shows the computational domain and the interface. Table 4 is the grid refinement analysis. Second order convergence again is verified.

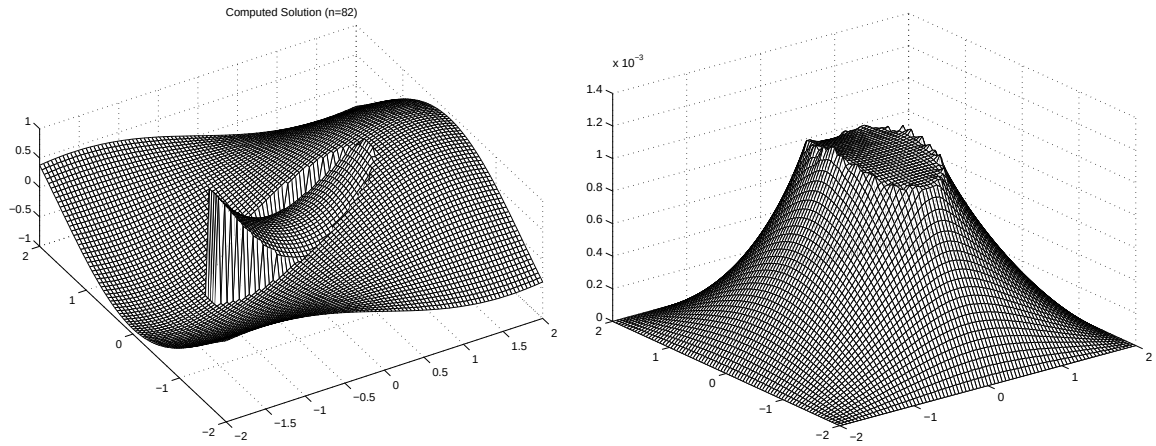


Figure 6: (a). The solution of Example 6.2 with jumps in the solution as well as in the normal derivatives. The parameters are $\beta^+ = 1$, $\beta^- = 100$, and $n_{finest} = 82$. (b). The error plot with the same parameters. The error distribution is better than that obtained from the original immersed interface method.

| $n_{finest}$ | $n_1$ | level | $n_{coarse}$ | $\| E_n \|_\infty$ | order |
|---|---|---|---|---|---|
| 42 | 40 | 4 | 6 | $2.4858\ 10^{-2}$ | |
| 82 | 80 | 5 | 6 | $3.3258\ 10^{-3}$ | 3.0065 |
| 162 | 160 | 6 | 6 | $4.9338\ 10^{-4}$ | 2.8026 |
| 322 | 320 | 7 | 6 | $1.2191\ 10^{-4}$ | 2.0351 |

Table 4: Numerical results of the second order method for Example 6.3 with $\beta^- = 1$ and $\beta^+ = 1000$, second order convergence is observed.

## 6.2 Algorithm efficiency analysis

A natural concern about the new methods proposed in this paper is how much extra cost needed in solving the quadratic optimization problem at each irregular grid point. In Fig. 8 we plot the percentage of the computational time used in the interface treatment versus the ratio of the jump in the coefficients. The cost for dealing with the irregular grid points includes solving the quadratic optimization problem, interpolating the cubic spline, indexing the irregular grid points, and finding $(x_i^*, y_j^*)$. For regular problems, the multigrid solver is as fast as the FFT fast Poisson solver and a little bit fast than the ADI (alternating directional implicit) method for Poisson equations. Therefore the multigrid method that we used is indeed a fast solver. In all our simulations, the cost for dealing with the irregular grid points near on the interface is less than 10%. When $\beta^- = \beta^+$, the finite difference coefficients become the standard five point stencil scheme and the cost for the interface treatment reaches its minimum.

The CPU time used in the entire solution process depends on the geometry and the jump in the coefficients. Table 5 lists some statistics for Example 6.2 on IBM SP2 machine. Below is a typical complete output.

```
n = 514,  n1 = 640,  beta- = 1000,  beta+ = 1,
```

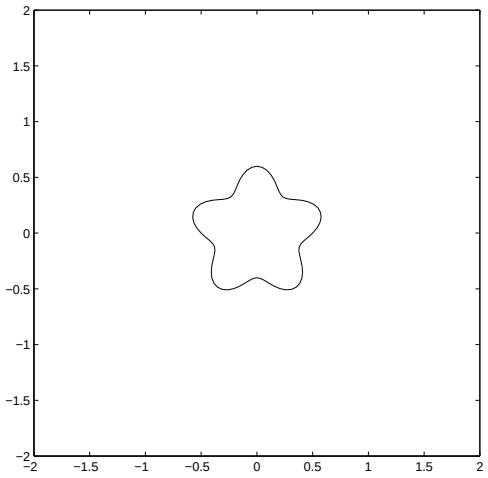


Figure 7: The computational domain and the interface for Example 6.3.

```
level = 7,  ncoarse = 9, error = 0.35424260271548154 2E-04
12.8u 0.6s 0:35 37% 211+51816k 0+0io 4pf+0w
```

We can see that for the large problem $514 \times 514$ with big jump in the coefficients, the CPU time needed is within a second.

| $n_{finest}$ | $n_1$ | level | $n_{coarse}$ | $\beta^-$ | $\beta^+$ | CPU time (s) |
|---|---|---|---|---|---|---|
| $258 \times 258$ | 320 | 6 | 9 | 1 | 1000 | 0.04 |
| $514 \times 514$ | 640 | 7 | 9 | 1 | 1000 | 0.15 |
| $514 \times 514$ | 640 | 7 | 9 | 1000 | 1 | 0.35 |

Table 5: CPU time for Example 6.2 with different parameters using IBM SP2 machine.

**Remark 6.1** It seems that the convergence of the multigrid solver depends on the jump in the coefficient and the mesh size. Therefore for piecewise constant coefficient $\beta$, the fast solver proposed in [20] may be a better choice since the number of iterations of the fast solver proposed in [20] is independent of the jump and the mesh size.

**Remark 6.2** The linear system of equations using the finite difference methods proposed in this paper is irreducible and diagonally dominant. The multigrid solver DMGD9V is designed for the finite difference method of standard nine-point stencil but not specifically for interface problems. Generally the multigrid method converges very fast for our method. However, we do observe occasionally that the multigrid stops before it returns a convergent result. In these cases, we still can make the multigrid method work by changing some built-in parameters such as the number of maximum iterations on the coarse grid, the number of smoothing operations etc. Other DMGD9V users[3] have had the same experiences.

[3]Private communication with Dr. X. Wu from Caltech and Exxon Company.

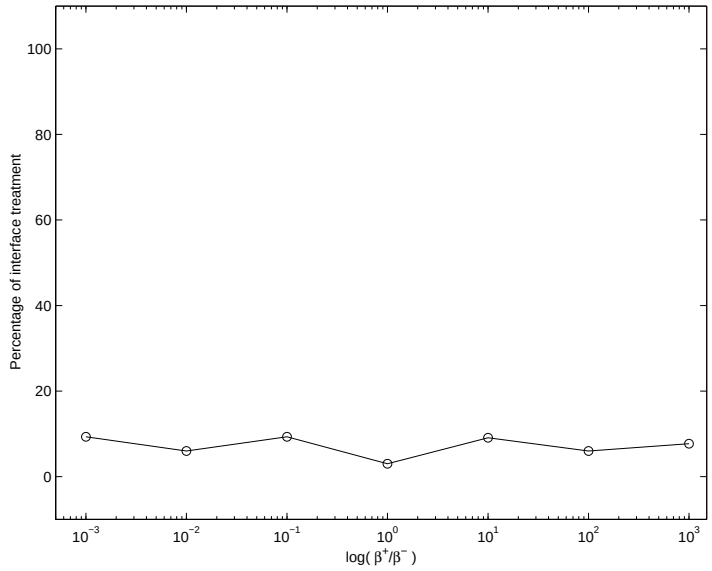


Figure 8: Percentage of the CPU time used for dealing with interfaces.

# 7 Conclusions

In this paper, we have proposed a class of finite difference methods that preserve the discrete maximum principles for elliptic interface problems. The convergence of the methods have been provided. The methods can be easily generalized to parabolic interface problems. We would strongly recommend the second order method over the first order method. A Fortran package for a single closed interface and the Dirichlet boundary condition is available upon request (zhilin@math.ncsu.edu).

# Acknowledgments.

We would like to thank K. Schittkowski for his quadratic optimization code and P. de Zeeuw for his multigrid solver. We are also grateful for the discussion with them and L. Adams and R. LeVeque.

The authors are partially supported an ARO grant, 39676-MA, and an NSF grant, DMS-96-26703, and North Carolina State FR&PD Fund.

## References


[1] L. M. Adams. A multigrid algorithm for immersed interface problems. pages 1–14. Proceedings of Copper Mountain Multigrid Conference, NASA Conference Publication 3339, 1995.

[2] I. Babuška. The finite element method for elliptic equations with discontinuous coefficients. *Computing*, 5:207–213, 1970.

[3] M. J. Berger and R. J. LeVeque. Adaptive mesh refinement using wave-propagation algorithms for hyperbolic systems. *SIAM J. Numer. Anal.*, 35:2298–2316, 1998.

[4] R. P. Beyer and R. J. LeVeque. Analysis of a one-dimensional model for the immersed boundary method. *SIAM J. Numer. Anal.*, 29:332–364, 1992.

[5] D. Calhoun. *A Cartesian grid method for solving the streamfunction-vorticity equations in irregular geometries.* PhD thesis, University of Washington, 1999.

[6] Z. Chen and J. Zou. Finite element methods and their convergence for elliptic and parabolic interface problems. *Numer. Math.*, 79:175–202, 1998.

[7] D. Colton and R. Kress. *Inverse Acoustic and Electromagnetic Scattering Theory.* Springer-Verlag, 1992.

[8] D. De Zeeuw. Matrix-dependent prolongations and restrictions in a blackbox multigrid solver. *J. Comput. Appl. Math.*, 33:1–27, 1990.

[9] A. L. Fogelson and J. P. Keener. Immersed interface methods for Neumann and related problems in two and three dimensions. *Submitted to SIAM J. Numer. Anal.*, 1997.

[10] L. Greengard and V. Rokhlin. A fast algorithm for particle summations. *J. Comput. Phys.*, 73:325–348, 1987.

[11] T. Hou, Z. Li, S. Osher, and H. Zhao. A hybrid method for moving interface problems with application to the Hele-Shaw flow. *J. Comput. Phys.*, 134:236–252, 1997.

[12] H. Huang and Z. Li. Convergence analysis of the immersed interface method. *IMA J. Numer. Anal.*, 19:583–608, 1999.

[13] J. Hunter, Z. Li, and H. Zhao. Autophobic spreading of drops,. NCSU CRSC-TR99-31, 1999.

[14] R. J. LeVeque. Clawpack and Amrclaw – Software for high-resolution Godunov methods. 4-th Intl. Conf. on Wave Propagation, Golden, Colorado, 1998.

[15] R. J. LeVeque and Z. Li. The immersed interface method for elliptic equations with discontinuous coefficients and singular sources. *SIAM J. Numer. Anal.*, 31:1019–1044, 1994.

[16] R. J. LeVeque and C. Zhang. Immersed interface methods for wave equations with discontinuous coefficients. *Wave Motion*, 25:237–263, 1997.

[17] R.J. LeVeque and Z. Li. Immersed interface method for Stokes flow with elastic boundaries or surface tension. *SIAM J. Sci. Comput.*, 18:709–735, 1997.

[18] Z. Li. *The Immersed Interface Method — A Numerical Approach for Partial Differential Equations with Interfaces.* PhD thesis, University of Washington, 1994.

[19] Z. Li. A note on immersed interface methods for three dimensional elliptic equations. *Computers Math. Appl.*, 31:9–17, 1996.

[20] Z. Li. A fast iterative algorithm for elliptic interface problems. *SIAM J. Numer. Anal.*, 35:230–254, 1998.

[21] Z. Li, T. Lin, and X. Wu. New Cartesian grid methods for interface problem using finite element formulation. *NCSU CRSC-TR99-5*, 1999.

[22] Z. Li and B. Soni. Fast and accurate numerical approaches for Stefan problems and crystal growth. *Numerical Heat Transfer, B: Fundamentals*, 35:461–484, 1999.

[23] Z. Li, H. Zhao, and H. Gao. A numerical study of electro-migration voiding by evolving level set functions on a fixed cartesian grid. *J. Comput. Phys.*, 152:281–304, 1999.

[24] X. Liu, R. Fedkiw, and M. Kang. A boundary condition capturing method for poisson's equation on irregular domain. UCLA CAM report #99-15, 1999.

[25] A. Mayo. The fast solution of Poisson's and the biharmonic equations on irregular regions. *SIAM J. Numer. Anal.*, 21:285–299, 1984.

[26] A. Mayo and A. Greenbaum. Fast parallel iterative solution of Poisson's and the biharmonic equations on irregular regions. *SIAM J. Sci. Stat. Comput.*, 13:101–118, 1992.

[27] A. McKenney, L. Greengard, and Anita Mayo. A fast poisson solver for complex geometries. *J. Comput. Phys.*, 118, 1995.

[28] K. W. Morton and D. F. Mayers. *Numerical Solution of Partial Differential Equations.* Cambridge press, 1995.

[29] S. Osher and J.A. Sethian. Fronts propagating with curvature-dependent speed: Algorithms based on Hamilton-Jacobi formulations. *J. Comput. Phys.*, 79:12–49, 1988.

[30] C. S. Peskin. Numerical analysis of blood flow in the heart. *J. Comput. Phys.*, 25:220–252, 1977.

[31] C. S. Peskin. Lectures on mathematical aspects of physiology. *Lectures in Appl. Math.*, 19:69–107, 1981.

[32] Paul N. Swarztrauber. Fast Poisson solver. In *Studies in Numerical Analysis,* G. H. Golub, editor, volume 24, pages 319–370. MAA, 1984.

[33] A. Wiegmann. *The explicit jump immersed interface method and interface problems for differential equations.* PhD thesis, University of Washington, 1998.

[34] A. Wiegmann and K. Bube. The immersed interface method for nonlinear differential equations with discontinuous coefficients and singular sources. *SIAM J. Numer. Anal.*, 35:177–200, 1998.

[35] D. Yang. Finite elements for elliptic interface problems with discontinuous coefficients and solutions. preprint, 1999.

# 8 Appendix: Relation to an intergral equation.

In this appendix, we show how the solution of the interface problem is associated with an integral equation.

Let $\Gamma$ be a closed $C^2$ curve, and the coefficient of $\beta$ is piecewise constant. Consider the interface Poisson problem defined on the infinite domain $R^d$

$$\begin{aligned} \nabla \cdot \beta \nabla u &= 0, \\ [u] = 0, \qquad & [\beta u_n] = V(s), \end{aligned}$$

where $V(s) \in C^{0,\alpha}(\Gamma)$, $0 < \alpha < 1$ is a function defined on the interface $\Gamma$. We represent the solution $u$ by the single-layer potential

$$u(\mathbf{x}) = \frac{1}{2\pi} \int_\Gamma G(\mathbf{x}, \mathbf{y}) \phi(\mathbf{y}) \, d\mathbf{y},$$

where $G$ is the Green's kernel function ($G(\mathbf{x}, \mathbf{y}) = log(|\mathbf{x} - \mathbf{y}|)$ for $R^2$). It follows from [7] that if $\phi \in C^{0,\alpha}(\Gamma)$, Hölder continous with exponent $\alpha$, then $u$ is continuous across $\Gamma$ and piecewise $C^{1,\alpha}$.

We determine $\phi$ so that the flux jump condition is satisfied. From the potential limiting theory [7], we have

$$u_n^{\pm}(s) = \frac{1}{2\pi} \int_\Gamma \frac{\partial}{\partial n_x} G(\mathbf{x}, \mathbf{y}) \phi(\mathbf{y}) \, dy \pm \frac{\mu(s)}{2}.$$

Define the integral operator $K$ by

$$K\phi = \frac{1}{2\pi} \int_\Gamma \frac{\partial}{\partial n_x} G(\mathbf{x}, \mathbf{y}) \phi(\mathbf{y}) \, d\mathbf{y}.$$

Note that

$$\begin{aligned} [\beta u_n](s) &= \beta^+ u_n^+ - \beta^- u_n^- \\ &= \beta^+ u_n^+ - \beta^+ u_n^- + \beta^+ u_n^- - \beta^- u_n^- \\ &= \beta^+ [u_n] + [\beta] u_n^- \\ &= \beta^+ \phi + [\beta](-\tfrac{\phi}{2} + K\phi) \end{aligned}$$

Therefore we get an integral equation for $\phi(s)$:

$$\left(\beta^+ - \frac{[\beta]}{2}\right) \phi + K\phi = V(s)$$

This is a Fredholm integral equation of the second kind. It has a unique solution $C^{0,\alpha}(\Gamma)$ provided that $V \in C^{0,\alpha}(\Gamma)$ [7] by the Riesz-Fredholm theory.